Impaired podocyte autophagy exacerbates proteinuria in diabetic nephropathy

Short running title: Podocyte autophagy in diabetic nephropathy

Atsuko Tagawa,[1,9] Mako Yasuda,[1,9] Shinji Kume,[1] Kosuke Yamahara,[1] Jun Nakazawa,[1] Masami Chin-Kanasaki,[1] Hisazumi Araki,[1] Shin-ichi Araki,[1] Daisuke Koya,[2] Katsuhiko Asanuma,[3,4] Eun-Hee Kim,[4,5] Masakazu Haneda,[6] Nobuyuki Kajiwara,[7] Kazuyuki Hayashi,[7] Hiroshi Ohashi,[8] Satoshi Ugi,[1] Hiroshi Maegawa,[1] Takashi Uzu[1]

[1] Department of Medicine, Shiga University of Medical Science, Otsu, Shiga, Japan.
[2] Division of Diabetology and Endocrinology, Kanazawa Medical University, Kahoku-Gun, Ishikawa, Japan.
[3] Laboratory for Kidney Research (TMK Project), Medical Innovation Center, Kyoto University Graduate School of Medicine, Sakyo-ku, Kyoto, Japan.
[4] Division of Nephrology, Juntendo University Faculty of Medicine, Bunkyo-ku, Tokyo, Japan.
[5] Osong Medical Innovation Foundation, Laboratory Animal Center, Cheongwon-gun, Chungbuk, Republic of Korea.
[6] Division of Metabolism and Biosystemic Science, Department of Internal Medicine, Asahikawa Medical University, Hokkaido, Japan.
[7] Department of Nephrology, Ikeda City Hospital, Ikeda, Osaka, Japan.
[8] Department of Pathology, Ikeda City Hospital, Ikeda, Osaka, Japan.
[9] These authors contributed equally to this work.

Corresponding author: Shinji Kume, M.D., Ph.D.
Department of Medicine, Shiga University of Medical Science,
Tsukinowa-Cho, Seta, Otsu, Shiga 520-2192, Japan.
Tel: +81-775-48-2222
Fax: +81-775-43-3858
Email: skume@belle.shiga-med.ac.jp

Word count: 4,000
Number of Figures: 8
Number of Tables: 0
Number of Supplemental Table: 2

Abstract

Overcoming refractory massive proteinuria remains a clinical and research issue in diabetic nephropathy. This study was designed to investigate the pathogenesis of massive proteinuria in diabetic nephropathy, with a special focus on podocyte autophagy, a system of intracellular degradation that maintains cell and organelle homeostasis, using human tissue samples and animal models. Insufficient podocyte autophagy was observed histologically in diabetic patients and rats with massive proteinuria accompanied by podocyte loss, but not in those with no or minimal proteinuria. Podocyte-specific autophagy-deficient mice developed podocyte loss and massive proteinuria in a high-fat diet (HFD)-induced diabetic model for inducing minimal proteinuria. Interestingly, huge damaged lysosomes were found in the podocytes of diabetic rats with massive proteinuria and HFD-fed podocyte-specific autophagy-deficient mice. Furthermore, stimulation of cultured podocytes with sera from diabetic patients and rats with massive proteinuria impaired autophagy, resulting in lysosome dysfunction and apoptosis. These results suggest that autophagy plays a pivotal role in maintaining lysosome homeostasis in podocytes under diabetic conditions, and that its impairment is involved in the pathogenesis of podocyte loss leading to massive proteinuria in diabetic nephropathy. These results may contribute to the development of new therapeutic strategy for advanced diabetic nephropathy.

Diabetic nephropathy is a leading cause of end-stage renal disease and is becoming a serious health problem worldwide. The appearance of microalbuminuria, the progression to overt proteinuria and the resultant renal dysfunction over several years to decades is the typical progressive course of diabetic nephropathy. Recent clinical studies have shown that microalbuminuria and a part of overt proteinuria can be halted and reversed by strict control of glycemia and blood pressure (1-3). However, some diabetic patients still develop massive proteinuria, resulting in a rapid decline of renal function (4). Thus, a better understanding of the pathogenesis of massive proteinuria in diabetic nephropathy may further improve renal outcomes in diabetic patients.

During evolution, living organisms developed several systems to overcome starvation in times of scarcity. These systems may be associated with the pathogenesis of diabetes and its vascular complications in times of plenty. Autophagy is an evolutionarily conserved intracellular catabolic process that allows for the degradation of proteins and organelles via the lysosomal pathway (5; 6). One major role of autophagy is to degrade proteins and reconstitute the intracellular metabolism to cope with starvation, and another is to remove damaged organelles such as mitochondria, peroxisomes and lysosomes (5-8). Autophagy is thus essential to maintain cell homeostasis under various stress conditions. Furthermore, autophagy has been shown to regulate whole-body glucose and lipid metabolisms in mammals, with impaired autophagy involved in the pathogenesis of several metabolic diseases (9-12). However, the role of autophagy in the pathogenesis of diabetic nephropathy remains unclear.

Podocytes are pivotal in maintaining glomerular filtration barrier function; thus, alterations in these cells are associated with massive proteinuria (13; 14). Podocytes are well-differentiated cells with no capacity to divide. The intracellular degradation system

is thus believed to be important in maintaining podocyte homeostasis. Indeed, clinical and experimental evidence has shown that lysosome dysfunction leads to severe podocyte injury and massive proteinuria (15-17). Interestingly, autophagy activity in podocytes is constitutively high, even under non-stress conditions (18; 19), suggesting that autophagy-lysosome system plays a pivotal role in maintaining podocyte homeostasis and that its alterations is involved in the pathogenesis of diabetic nephropathy.

Thus, this study was designed to determine the role of autophagy in maintaining podocyte homeostasis under diabetic condition and its involvement in the development of massive proteinuria in diabetic nephropathy.

Research Design and Methods

Study approvals. All procedures in the animal studies were performed in accordance with the guidelines of the Research Center for Animal Life Science of Shiga University of Medical Science. In human studies, all patients provided written informed consent. The protocols for human studies were approved by the Scientific-Ethical Committees of Shiga University of Medical Science and Ikeda City Hospital, and adhered to the Declaration of Helsinki guidelines.

Kidney biopsy specimens. Human kidney biopsy specimens were obtained from seven type 2 diabetic patients with massive proteinuria (> 3.5 g/d), four type 2 diabetic patients with minimal proteinuria (< 0.5 g/d), six patients with membranous nephropathy with reversible nephrotic-range proteinuria, three patients with minimal change nephrotic syndrome with reversible nephrotic-range proteinuria, and five

patients with IgA nephropathy with minimal proteinuria. All diabetic patients had diabetes for over 10 years as well as retinopathy.

Diabetic rodent models. Eight-week-old male C57BL/6 mice were obtained from Clea Japan Inc. (Tokyo, Japan), and 8-week-old Long-Evans Tokushima Otsuka (LETO) and Otsuka Long-Evans Tokushima fatty (OLETF) rats from Shimizu Laboratory Supplies Co., Ltd. (Kyoto, Japan). The mice were fed either a standard (STD; 10% of total calories from fat) or a high-fat (HFD; 60% of total calories from fat) diet for 32 weeks. LETO and OLETF rats were fed ad-libitum until 50-week-old, although some OLETF rats were sacrificed at age 32 weeks. The rodents were fasted overnight and sacrificed (20).

In vivo autophagy analysis. GFP-LC3 transgenic mice provided by Noboru Mizushima (Tokyo University, Japan) were used to analyze autophagy activity (19).

HFD-induced diabetes in podocyte-specific autophagy-deficient mice. Podocyte-specific *Atg5*-deficient mice (Podo-Atg5$^{-/-}$) were generated by crossbreeding Atg5$^{f/f}$ mice (21) with *Nphs2-Cre* transgenic mice (22). Eight-week-old male Atg5$^{f/f}$ mice were used as a control group. All mice were crossed on C57BL/6 background. To assess the effects of dietary intervention, Podo-Atg5$^{f/f}$ mice were fed a STD (n = 5) or HFD (n = 6), and Podo-Atg5$^{-/-}$mice were fed a STD (n = 7) or HFD (n = 9), for 32 weeks (23).

Blood and urine analysis. Blood glucose concentrations were measured using a Glutest sensor (Sanwa Kagaku, Nagoya, Japan). Plasma insulin was measured by ELISA (Morinaga, Tokyo, Japan). Urinary albumin excretion was measured by immunoblot and ELISA (Exocell, Philadelphia, PA) (20). Glucose and insulin tolerance tests were performed as previously reported (23).

Histological analyses. Fixed kidney specimens embedded in paraffin were sectioned at 3 μm thickness. Antibodies to p62 (MBL, Tokyo, Japan), fibronectin (Chemicon, Temecula, CA), F4/80 (Serotec, Oxford, UK), WT1 (Santa Cruz Biotechnology, CA), podocin (Sigma, St. Louis, MO), synaptopodin (Progen, Heidelberg, Germany), lamp2 (Abcam, Cambridge, UK), and ubiquitin (Cell Signaling Technology, Beverly, MA) were used. Transmission and scanning electron microscopic analysis were performed with the Hitachi S-570 and H-7500 (Hitachi, Tokyo, Japan). For semi-quantitative analysis of p62 accumulation, the glomerular intensity of staining was rated as grades 1 (none), 2 (minor), 3 (moderate), 4 (severe), and 5 (most severe) (20). More than 10 glomeruli in each mouse or human samples were evaluated. To determine podocyte number, serial kidney sections were stained with WT1 antibody, and WT1-positive cells were counted, with the number calculated using the dissector/fractionator combination method (24-26). Histological analyses were performed by three independent nephrologists in a blinded manner.

Western blot analysis. Western blot analysis was performed as described (20). The membranes were incubated with antibodies against cleaved caspase 3 (Asp175), ubiquitin and Atg7 (Cell Signaling Technology; Beverly, MA), LC3 (Novus

Biologicals; Littleton, CO), β actin (Sigma, St. Louis, MO), and p62 (MBL, Tokyo Japan).

Cell culture. The mouse podocyte cell line was cultured as described (27; 28). Differentiated cells were stimulated with high glucose (500 mg/dl), fatty acids (palmitate and oleate, 150 μM each), tumor necrosis factor-α (TNFα, 10 ng/μl) or serum for 24 hours. Sera were collected from the indicated rodent models and patients. Complement was depleted by heat-inactivation, and cells were incubated 10% serum for 24 hours (29; 30), with/without lysosome inhibitors for 1 hour (31). Characteristics of the sera used in this study are shown in Supplemental Table 1 and 2.

Generation of Immortalized Atg7-deficient podocyte cell line. Immortalized *Atg7*-deficient podocyte cell line was generated with pMESVTS plasmid containing a SV40 large T antigen (32). Glomeruli of podocyte-specific Atg7-deficient (33; 34) and wild-type mice were isolated using Dynabeads M-450 tosylactivated (Invitrogen, Carlsbad, CA) (35). Podocytes were infected with viral supernatant from PLAT-E cells transfected with pMESVTS plasmid (36), and were maintained in RPMI-1640 with 10% fetal bovine serum at 33 ℃. The cells were cultured at 39 ℃ to induce differentiation over 7 days.

Human serum samples. Human serum samples were taken from patients with type 2 diabetes mellitus in the Shiga Prospective Observational Follow-up Study in 2011 and 2012 (2). The preliminary study included 11 patients, three with normoalbuminuria (< 30 mg/gCre), three with microalbuminuria (30-300 mg/gCre), two with

macroalbuminuria (> 300 mg/gCre), and three with massive proteinuria (> 3.5 g/gCre). The validation study included 50 subjects, 10 non-diabetic subjects and 40 type 2 diabetic patients, including 10 with normoalbuminuria, 11 with microalbuminuria, 10 with macroalbuminuria, and nine with massive proteinuria (Supplemental Table 2). ELISA was used to measure the concentrations of p62 (Enzo Life Science, Farmingdale, NY).

Statistical analyses. Results are expressed as the mean ± SEM. ANOVA and a subsequent Tukey's test were used to determine the significance of differences in multiple comparisons. Student's t test was used for comparisons of two groups. A *P* value < 0.05 was considered statistically significant.

Results

Insufficient autophagy in podocytes of diabetic patients with massive proteinuria. To examine the relationships among levels of proteinuria, podocyte damage and autophagy, kidney biopsy samples taken from patients with diabetic nephropathy and refractory massive proteinuria (> 3.5 g/day; Fig. 1A, Patients 1–7) or minimal proteinuria (< 0.5 g/day; Fig. 1C, Patients 17–20), membranous nephropathy and minima change with reversible massive proteinuria (Fig. 1B, Patients 8–16) and IgA nephropathy with minimal proteinuria (Fig. 1C, Patients 21–25) were analyzed. Mesangial expansion in periodic acid-Schiff (PAS) staining were observed in all patients with diabetic nephropathy, regardless of proteinuria level (Fig. 1A, Patients 1–7 and Fig. 1C, 17–20). To examine podocyte injury, we conducted immunofluorescent study for podocin protein that is a key protein of the slit diaphragm of podocytes (14).

The podocin expression pattern was nearly normal in the patients with minimal proteinuria, whether or not they had diabetic nephropathy (Fig. 1C, Patients 17–25). In contrast, the podocin expression pattern was granular and irregularly scattered in the patients with massive proteinuria regardless of the underlying disease (Fig. 1A and B, Patients 1–16). In addition, decreases in podocin-positive areas were obviously observed in the patients with refractory massive proteinuria due to diabetes (Fig. 1A, Patients 1–7).

The protein p62 is a specific target of the autophagy degradation; thus, intracellular accumulation of this protein is indicative of insufficient autophagy (37). Intense accumulation of p62 protein was significantly increased in the glomeruli of the diabetic patients with massive proteinuria (Fig. 1A–D).

Insufficient autophagy and podocyte injury in diabetic rodents with massive proteinuria. We further confirmed the relationship among disease stage of diabetic nephropathy, podocyte injury and autophagy insufficiency, by utilizing two rodent models of diabetic nephropathy. One model, in mice, involved HFD-induced renal injury, resulting in diabetes-associated minimal proteinuria (23; 38). The second model involved OLETF rats, which spontaneously develop hyperglycemia and subsequent massive proteinuria with age (39). Western blot analysis of urine samples and PAS staining showed minimal proteinuria with glomerular hypertrophy in HFD-fed C57BL/6 mice, and age-dependent progression of proteinuria with glomerular sclerosis in OLETF rats (Figs. 2A-C). Podocytes in 50-week-old OLETF rats with massive proteinuria showed a reduction in podocin-positive areas, with severe alterations in foot processes

and p62 accumulation (Fig. 2C and E). However, these alterations were not found in the other rodent models (Fig. 2C, D and E).

Exacerbation of HFD-induced albuminuria in podocyte-specific autophagy-deficient mice. These histological results showed that insufficient podocyte autophagy was associated with severe podocyte injury and massive proteinuria in diabetes. To assess the causal association, we used podocyte-specific autophagy-deficient mice.

The protein coded by the *Atg5* gene is essential for autophagosome formation (21). Thus, podocyte-specific autophagy-deficient mice were generated by crossbreeding $Atg5^{f/f}$ mice (21) with *Nphs2*-Cre transgenic mice (22). Microtubule-associated protein 1 light chain 3 (LC3), a regulatory protein essential for the induction of autophagy, localizes to autophagosome membranes during activation of autophagy. Thus, autophagy activity in cells of GFP-LC3 transgenic mice can be monitored as green dots (19). Impaired formation of GFP-LC3 dots was confirmed in the podocytes of podocyte-specific Atg5-knockout mice (podo-$Atg5^{-/-}$) crossbred with GFP-LC3 transgenic mice (Fig. 3A).

To assess the effects of podocyte autophagy deficiency on HFD-induced minimal proteinuria, control $Atg5^{f/f}$ and podo-$Atg5^{-/-}$ mice were fed a STD or a HFD for 32 weeks. During 32 weeks, HFD-fed $Atg5^{f/f}$ and podo-$Atg5^{-/-}$ mice showed similar development of obesity, hyperinsulinemic hyperglycemia, glucose intolerance and insulin resistance (Figs. 3B-H). HFD-fed $Atg5^{f/f}$ mice developed minimal albuminuria, and STD-fed podo-$Atg5^{-/-}$ mice did not show increased urinary albumin excretion (Figs.

3I and J). However, HFD-fed podo-Atg5$^{-/-}$ mice developed massive albuminuria (Figs. 3I and J).

Exacerbation of proteinuria-related tubulointerstitial lesions in HFD-fed podocyte-specific autophagy-deficient mice. Histological analysis of the glomeruli of Atg5$^{f/f}$ mice showed that the HFD increased glomerular size, PAS-positive area and fibronectin deposition in glomeruli (Figs. 4A and B). These HFD-induced glomerular alterations tended to be greater in podo-Atg5$^{-/-}$ than in Atg5$^{f/f}$ mice, but the differences were not statistically significant (Figs. 4A and B). In contrast, renal tubulointerstitial lesions, as determined by H&E staining and immunohistochemical analysis of F4/80-positive macrophage, were exacerbated in HFD-fed podo-Atg5$^{-/-}$ mice (Figs. 4C and D), suggesting that podocyte-specific autophagy insufficiency under diabetic conditions resulted in massive proteinuria, accompanied by proteinuria-induced tubulointerstitial damage.

There was no evidence of p62 accumulation in the podocytes of HFD-fed Atg5$^{f/f}$ mice, and GFP-LC3 dot formation was not altered in the podocytes of HFD-fed GFP-LC3 mice (Figs. 4E-H), suggesting that HFD-induced diabetes alone did not affect podocyte autophagy and that autophagy was not related to the onset of HFD-induced minimal proteinuria. In contrast, p62 accumulation was significantly higher in the podocytes of HFD-fed podo-Atg5$^{-/-}$ mice with massive proteinuria (Figs. 4E and F). These results suggested that insufficient autophagy played a causal role in the progression of proteinuria, from minimal to massive levels, under diabetic conditions.

Podocyte damage in HFD-fed podocyte-specific autophagy-deficient mice.

Transmission electron microscopy showed that both Atg5$^{f/f}$ and podo-Atg5$^{-/-}$ mice fed the HFD for 32 weeks resulted in thickening of the glomerular basement membrane (Fig. 5A). STD-fed podo-Atg5$^{-/-}$ mice showed nearly normal podocyte morphology, whereas HFD-fed podo-Atg5$^{-/-}$ mice developed severe foot process effacement (Fig. 5A). Furthermore, in scanning electron microscopy, normal foot process structure was drastically disrupted in the podocytes of HFD-fed podo-Atg5$^{-/-}$ mice (Fig. 5B).

The podocin expression pattern was normally and linearly aligned in STD- and HFD-fed Atg5$^{f/f}$ mice and in STD-fed podo-Atg5$^{-/-}$ mice (Fig. 5C). However, the pattern was visible as dots in HFD-fed podo-Atg5$^{-/-}$ mice (Fig. 5C), similar to that observed in diabetic patients with massive proteinuria. Podocin internalization is an additional marker of alterations in podocyte foot processes (40). Most podocin (red) and synaptopodin (green) signals were visible as normal capillary pattern in the undamaged podocytes of STD- and HFD-fed Atg5$^{f/f}$ mice and STD-fed podo-Atg5$^{-/-}$ mice (Fig. 5D). In contrast, increased podocin internalization, as shown by the increased podocin expression in cytosol and the merged yellow signals, was observed in the damaged podocytes of HFD-fed podo-Atg5$^{-/-}$ mice (Fig. 5D). In addition, the number of WT1-positive podocyte number was significantly reduced in HFD-fed podo-Atg5$^{-/-}$ mice (Figs. 5E and F). These results suggested that autophagy insufficiency combined with diabetic conditions caused podocyte damages.

Insufficient autophagy-related apoptosis in cultured podocytes stimulated with serum from diabetic rodents. High glucose, fatty acids and TNFα, an inflammatory cytokine, are major pathogenic factors in diabetic nephropathy. However, each of these, as well as their combination, had no effect on autophagy activity, as determined by p62

accumulation and LC3II conversion in cultured podocytes (Fig. 6A–C), suggesting that other factors may alter autophagy in podocytes. Several reports showed that some serum factors altered intracellular signaling pathways and autophagy activity in some conditions (29; 30), raising a possibility that some serum factors associated with diabetic massive proteinuria might inhibit autophagy in podocytes.

To determine this possibility, mouse podocytes were cultured with serum from STD- or HFD-fed C57BL/6 mice or 50-week-old LETO or OLETF rats, and LC3 dot formation was assessed by immunofluorescence (Fig. 6D, protocol 1). LC3 dot formation was lower in cultured podocytes stimulated with serum from 50-week-old OLETF rats (Fig. 6E). Insufficient autophagy in cultured podocytes stimulated with serum from 50-week-old OLETF rats (Fig. 6D, protocol 2) was also confirmed by an increase in p62 expression levels and a decrease in LC3II bands (Fig. 6F and G). Furthermore, treatment with OLETF rat serum alone significantly enhanced apoptosis in normal podocytes, as shown by the cleavage of caspase 3 (Fig. 6F and G). These results suggested that some serum factors of 50 week-old OLETF rats inhibited autophagy and caused apoptosis in podocytes.

We excluded a possibility that serum alterations related to massive proteinuria secondarily caused autophagy insufficiency in podocytes. Stimulation with the serum from podo-Atg5$^{-/-}$ mice fed a HFD had no effect on both p62 accumulation and apoptosis in cultured podocytes (Fig. 6D, protocol 3 and 6H), even though they showed massive proteinuria, indicating that massive proteinuria-related serum alteration itself was not a cause of autophagy insufficiency.

To further examine causal relationship between autophagy insufficiency and apoptosis associated with diabetic serum, we used cultured Atg7-deficient podocytes.

The protein coded by the *Atg7* gene is also essential for autophagosome formation (33). Atg7 protein expression was not observed in cultured Atg7-deficient podocytes, and autophagy deficiency was confirmed by a significant increase in p62 protein and a decrease in LC3II bands (Fig. 6I). These cells were subsequently incubated with serum from STD- or HFD-fed C57BL/6 mice (Fig. 6D, protocol 4). Serum from HFD-fed C57BL/6 mice had no effect on the control $Atg7^{f/f}$ podocytes, whereas it significantly increased the cleavage of caspase 3 in the Atg7-deficient podocytes (Fig. 6I and J). The study provided further evidence that insufficient autophagy played a causal role in podocyte apoptosis under diabetic condition.

Accumulation of damaged lysosomes in the podocytes of diabetic rodents with massive proteinuria. To determine the intracellular component targeted by autophagy in podocytes under diabetic conditions, intracellular structural changes in the podocytes were analyzed. The podocytes of $Atg5^{f/f}$ mice had a normal mitochondrial structure with normal autophagosomes formation, regardless of diet (Fig. 7A). In the podocytes of STD-fed podo-$Atg5^{-/-}$ mice, autophagosomes were absent and unidentifiable deposits were observed, but mitochondrial structure and nuclear shape were normal (Fig. 7A). Interestingly, the cytosol in podocytes of HFD-fed podo-$Atg5^{-/-}$ mice was occupied by a number of huge balloon-like structures, suggesting damaged lysosomes (Fig. 7A).

Autophagy system is involved in removing damaged lysosomes and maintaining lysosome homeostasis (8; 41), raising a hypothesis that lysosomes damaged by diabetic metabolic loads were targets of autophagy, and that impairment of autophagy by diabetic conditions would result in the accumulation of damaged lysosomes (Fig. 7B). Actually, the levels of expression of lysosome-associated

membrane protein-2 (lamp2), a membrane marker of lysosomes (42), and ubiquitinated proteins to be degraded by lysosomes were increased in the podocytes of HFD-fed podo-Atg5$^{-/-}$ mice (Fig. 7C), suggesting that dysfunctional lysosomes accumulated in these podocytes. The accumulation of huge lysosomes with the increase in lamp2-positive areas and the absence of autophagosomes were observed in the podocytes of 50-week-old OLETF rats with massive proteinuria (Fig. 7D).

In addition, ubiquitinated proteins were found to accumulate in Atg7-deficient podocytes stimulated with the HFD mouse serum and normal podocytes stimulated with the 50-week-old OLETF rat serum (Fig. 7E). Furthermore, a double immunofluorescence assay for LC3 and lamp2 revealed a number of large lamp2-positive signals in these cells, with absent or impaired LC3 dot formation (Figs. 7F and G). These results confirmed our hypothesis, that systemic diabetic changes injure lysosomes, and that diabetic conditions accompanied by massive proteinuria additionally impair autophagy, leading to the accumulation of damaged lysosomes.

Insufficient autophagy in cultured podocytes stimulated with serum from diabetic patients with massive proteinuria. Finally, to determine the disease stage of human diabetic nephropathy associated with the impaired autophagy-lysosome system, the levels of p62 and ubiquitinated proteins were assessed in cultured podocytes stimulated with serum from 11 diabetic patients with a varying range of proteinuria. Stimulation of cultured podocytes with serum from diabetic patients with massive proteinuria resulted in increases in p62 and ubiquitinated protein (Fig. 8A).

To validate the relationship between proteinuria progression and autophagy-lysosome dysfunction in 10 non-diabetic subjects and 40 diabetic patients

with varying degrees of proteinuria (Supplemental Table 2), the accumulation of p62 protein in cultured podocytes stimulated with serum was assessed by ELISA (Fig. 8B). The levels of p62 protein was significantly higher in cultured podocytes stimulated with the serum from diabetic patients with massive proteinuria than with serum from other disease stages (Fig. 8C). Diabetes alone did not affect p62 accumulation in the cultured podocytes (Fig. 8C). These results suggested that insufficient autophagy was particularly associated with progression to massive proteinuria in human diabetic nephropathy.

Discussion

The results presented here have demonstrated that impaired autophagy in podocytes is involved in the pathogenesis of severe podocyte injury, leading to massive proteinuria in diabetic nephropathy. Furthermore, maintenance of lysosome homeostasis by removing damaged lysosomes may be a crucial task of podocyte autophagy under diabetic conditions.

During the past decade, autophagy has been intensively studied in animals with kidney diseases (43). Previous studies using podocyte- and proximal tubular cell-specific autophagy-deficient mice has shown that autophagy insufficiency is related to stress susceptibility (8; 44-47), suggesting that autophagy is essential for renoprotection against various pathogenic conditions. Because autophagy is regulated by both nutrients and stress signals, it has been speculated that autophagy is involved in the pathogenesis of diabetic nephropathy (48). The present study utilizing

podocyte-specific autophagy-deficient mice provide, for the first time, a strong evidence indicating that autophagy is involved in the pathogenesis of diabetic nephropathy.

Autophagy insufficiency was observed specifically in podocytes of diabetic patients and rodents with massive proteinuria, but not with the other disease stage. Furthermore, HFD-induced diabetes caused minimal proteinuria in mice with normal podocyte autophagy, but massive proteinuria with podocyte loss in mice with podocyte-specific autophagy-deficiency. These findings indicate that diabetes alone can cause typical glomerular changes leading to minimal proteinuria, whereas complicated impairment of podocyte autophagy during the course of diabetic nephropathy results in podocyte loss, followed by massive proteinuria (Fig. 8D). Thus, insufficient podocyte autophagy may play a pathogenic role particularly in the disease progression to massive proteinuria in diabetic nephropathy. However, this study had several limitations, which may have affected interpretation of the results. Autophagy deficiency was assessed only by p62 staining and electron microscopic analysis, the number of human kidney biopsy samples was small, and two different rodent species were compared: HFD-fed mice as a model of albuminuria and OLETF rats as a model of massive proteinuria. Additional methods of assessing autophagy deficiency and large clinical cohort and/or animal studies are needed to validate our conclusions.

The mechanism underlying diabetes-related impairment of podocyte autophagy is still unclear. Sera from patients and rodents with massive proteinuria impaired autophagy in cultured podocytes, suggesting that serum factors associated with massive proteinuria in diabetes, but not with diabetes per se, impair podocyte autophagy. The mammalian target of rapamycin complex 1 (mTORC1) is a nutrient-sensing signal that inhibits autophagy (49). Interestingly, mTORC1 activity has been reported to be

enhanced in podocytes of humans and animals with advanced diabetic nephropathy (50; 51), suggesting that some factors in diabetic serum may activate mTORC1, suppressing podocyte autophagy. Additional studies are required to identify these serum factors and intracellular molecular pathways that inhibit podocyte autophagy, and may contribute to the development of new therapy for the treatment of refractory diabetic nephropathy. Furthermore, the bioassay involving serum stimulation of cultured cells may be useful in assessing *in vivo* autophagy activity in human subjects and experimental animals.

Autophagy can degrade many damaged proteins and organelles (7). To date, however, the specific targets of podocyte autophagy have not been identified. Fabry disease, a lysosome disease, causes podocyte damage and proteinuria (15). Moreover, the deletion of a single gene that regulates lysosome function enhanced podocyte damage and proteinuria in mice (16; 17). These results indicate that lysosome is likely important in maintaining podocyte homeostasis. Interestingly, a massive accumulation of lysosomes with abnormal morphology was observed in the podocytes of diabetic rodents with autophagy deficiency. It remains unclear whether lysosome is also a target of podocyte autophagy under other pathogenic conditions. Our results, however, suggest that damaged lysosomes are an important degradation target of podocyte autophagy at least under diabetic conditions.

Clinically, there are few effective treatments for diabetic patients with massive proteinuria; thus, these patients often experience a rapid decline in renal function (4). Because proteinuria is the most likely cause of tubulointerstitial lesions that lead to renal dysfunction, new therapeutic agents are needed to halt the stage progression of proteinuria and/or to protect renal tubular cells against proteinuria-related renotoxicity, thus improving renal outcomes in patients with refractory diabetic nephropathy. We

recently reported that autophagy insufficiency in proximal tubular cells was associated with the pathogenesis of obesity- and diabetes-mediated exacerbation of proteinuria-induced tubulointerstitial damage (52). Taken together, our previous and present findings suggest that autophagy activation may be effective for diabetic patients with massive proteinuria and resultant rapid decline of renal function.

In conclusion, autophagy plays a pivotal role in maintaining lysosome homeostasis in podocytes under diabetic conditions. The impairment of autophagy is involved in the pathogenesis of podocyte loss, leading to massive proteinuria in diabetic nephropathy. These findings suggest a new therapeutic strategy for massive proteinuria in patients with diabetic nephropathy.

Acknowledgments

We thank Dr. P. Mundel (Harvard Medical School, Massachusetts General Hospital), Dr. N. Kobayashi (University of Ehime) and Dr. Y. Makino (Asahikawa Medical University) for kindly providing the cells and for their very helpful advice on cell cultures. We also thank Dr. N. Mizushima (Tokyo University) for donating the *Atg5*-floxed and GFP-LC3 transgenic mice, and Dr. T. Kitamura (Tokyo University) and Dr. M. Komatsu (Niigata University) for providing the PLAT-E cells and the pMESVTS plasmid. We are grateful to Y. Omura and N. Yamanaka (Shiga University of Medical Science); to H. Mukai, M. Kawai, M. Iwaki, and T. Kanemoto (Ikeda City Hospital); to the Central Research Laboratory of Shiga University of Medical Science for technical assistance; and to all members of the Maegawa Laboratory for their contributions to the Shiga Prospective Observational Follow-up Study.

Author contributions

A.T., M.Y., S.K., K.Y., K.A., E-H.K., and S.U. performed the experimental works. D.K., M.H., H.M. and T.U. gave conceptual advice. N.K., K.H., and H.O. collected human kidny biopsy samples. A.T., M.Y. and S.K. wrote the manuscript. J.N., M.C-K., H.A. and SI.A. contributed to the study concept and research design, and interpretation of the results. All authors contributed to discussion and reviewed/edited manuscript. S.K. is the guarantor of this work and, as such, had full access to all the data in the study and takes responsibility for the integrity of the data and the accuracy of the data analysis.

Conflict of interest statement

The authors declare no competing financial interests.

Funding

This study was supported by Grants-in-Aid for Scientific Research (KAKENHI) from the Japan Society for the Promotion of Science (No. 25713033 to S. K., No. 26293217 to H. M, No. 15K19511 to M.Y. and No. 26670431 to K. A.); from the Takeda Science Foundation (to S. K.); from the Banyu Life Science Foundation International (to S. K.); and from the Uehara Memorial Foundation (to S. K.).

References

1. Perkins BA, Ficociello LH, Silva KH, Finkelstein DM, Warram JH, Krolewski AS: Regression of microalbuminuria in type 1 diabetes. N Engl J Med 2003;348:2285-2293
2. Araki S, Haneda M, Sugimoto T, Isono M, Isshiki K, Kashiwagi A, Koya D: Factors associated with frequent remission of microalbuminuria in patients with type 2 diabetes. Diabetes 2005;54:2983-2987
3. Yokoyama H, Araki S, Honjo J, Okizaki S, Yamada D, Shudo R, Shimizu H, Sone H,

Moriya T, Haneda M: Association between remission of macroalbuminuria and preservation of renal function in patients with type 2 diabetes with overt proteinuria. Diabetes Care 2013;36:3227-3233
4. Rossing K, Christensen PK, Hovind P, Tarnow L, Rossing P, Parving HH: Progression of nephropathy in type 2 diabetic patients. Kidney Int 2004;66:1596-1605
5. Mizushima N, Komatsu M: Autophagy: renovation of cells and tissues. Cell 2011;147:728-741
6. Mizushima N, Levine B, Cuervo AM, Klionsky DJ: Autophagy fights disease through cellular self-digestion. Nature 2008;451:1069-1075
7. Kroemer G, Marino G, Levine B: Autophagy and the integrated stress response. Mol Cell 2010;40:280-293
8. Maejima I, Takahashi A, Omori H, Kimura T, Takabatake Y, Saitoh T, Yamamoto A, Hamasaki M, Noda T, Isaka Y, Yoshimori T: Autophagy sequesters damaged lysosomes to control lysosomal biogenesis and kidney injury. EMBO J 2013;32:2336-2347
9. Ebato C, Uchida T, Arakawa M, Komatsu M, Ueno T, Komiya K, Azuma K, Hirose T, Tanaka K, Kominami E, Kawamori R, Fujitani Y, Watada H: Autophagy is important in islet homeostasis and compensatory increase of beta cell mass in response to high-fat diet. Cell Metab 2008;8:325-332
10. Shigihara N, Fukunaka A, Hara A, Komiya K, Honda A, Uchida T, Abe H, Toyofuku Y, Tamaki M, Ogihara T, Miyatsuka T, Hiddinga HJ, Sakagashira S, Koike M, Uchiyama Y, Yoshimori T, Eberhardt NL, Fujitani Y, Watada H: Human IAPP-induced pancreatic beta cell toxicity and its regulation by autophagy. J Clin Invest 2014;124:3634-3644
11. Rabinowitz JD, White E: Autophagy and metabolism. Science 2010;330:1344-1348
12. Ezaki J, Matsumoto N, Takeda-Ezaki M, Komatsu M, Takahashi K, Hiraoka Y, Taka H, Fujimura T, Takehana K, Yoshida M, Iwata J, Tanida I, Furuya N, Zheng DM, Tada N, Tanaka K, Kominami E, Ueno T: Liver autophagy contributes to the maintenance of blood glucose and amino acid levels. Autophagy 2011;7:727-736
13. Shih NY, Li J, Karpitskii V, Nguyen A, Dustin ML, Kanagawa O, Miner JH, Shaw AS: Congenital nephrotic syndrome in mice lacking CD2-associated protein. Science 1999;286:312-315
14. Boute N, Gribouval O, Roselli S, Benessy F, Lee H, Fuchshuber A, Dahan K, Gubler MC, Niaudet P, Antignac C: NPHS2, encoding the glomerular protein podocin, is mutated in autosomal recessive steroid-resistant nephrotic syndrome. Nat Genet 2000;24:349-354
15. Kint JA: Fabry's disease: alpha-galactosidase deficiency. Science

1970;167:1268-1269
16. Oshima Y, Kinouchi K, Ichihara A, Sakoda M, Kurauchi-Mito A, Bokuda K, Narita T, Kurosawa H, Sun-Wada GH, Wada Y, Yamada T, Takemoto M, Saleem MA, Quaggin SE, Itoh H: Prorenin receptor is essential for normal podocyte structure and function. J Am Soc Nephrol 2011;22:2203-2212
17. Cina DP, Onay T, Paltoo A, Li C, Maezawa Y, De Arteaga J, Jurisicova A, Quaggin SE: Inhibition of MTOR disrupts autophagic flux in podocytes. J Am Soc Nephrol 2012;23:412-420
18. Asanuma K, Tanida I, Shirato I, Ueno T, Takahara H, Nishitani T, Kominami E, Tomino Y: MAP-LC3, a promising autophagosomal marker, is processed during the differentiation and recovery of podocytes from PAN nephrosis. FASEB J 2003;17:1165-1167
19. Mizushima N, Yamamoto A, Matsui M, Yoshimori T, Ohsumi Y: In vivo analysis of autophagy in response to nutrient starvation using transgenic mice expressing a fluorescent autophagosome marker. Mol Biol Cell 2004;15:1101-1111
20. Tanaka Y, Kume S, Araki S, Isshiki K, Chin-Kanasaki M, Sakaguchi M, Sugimoto T, Koya D, Haneda M, Kashiwagi A, Maegawa H, Uzu T: Fenofibrate, a PPARalpha agonist, has renoprotective effects in mice by enhancing renal lipolysis. Kidney Int 2011;79:871-882
21. Kuma A, Hatano M, Matsui M, Yamamoto A, Nakaya H, Yoshimori T, Ohsumi Y, Tokuhisa T, Mizushima N: The role of autophagy during the early neonatal starvation period. Nature 2004;432:1032-1036
22. Moeller MJ, Sanden SK, Soofi A, Wiggins RC, Holzman LB: Podocyte-specific expression of cre recombinase in transgenic mice. Genesis 2003;35:39-42
23. Deji N, Kume S, Araki S, Soumura M, Sugimoto T, Isshiki K, Chin-Kanasaki M, Sakaguchi M, Koya D, Haneda M, Kashiwagi A, Uzu T: Structural and functional changes in the kidneys of high-fat diet-induced obese mice. Am J Physiol Renal Physiol 2009;296:F118-126
24. Nyengaard JR: Stereologic methods and their application in kidney research. J Am Soc Nephrol 1999;10:1100-1123
25. White KE, Bilous RW, Marshall SM, El Nahas M, Remuzzi G, Piras G, De Cosmo S, Viberti G: Podocyte number in normotensive type 1 diabetic patients with albuminuria. Diabetes 2002;51:3083-3089
26. Lemley KV, Bertram JF, Nicholas SB, White K: Estimation of glomerular podocyte number: a selection of valid methods. J Am Soc Nephrol 2013;24:1193-1202
27. Mundel P, Reiser J, Zuniga Mejia Borja A, Pavenstadt H, Davidson GR, Kriz W,

Zeller R: Rearrangements of the cytoskeleton and cell contacts induce process formation during differentiation of conditionally immortalized mouse podocyte cell lines. Exp Cell Res 1997;236:248-258
28. Yasuda M, Tanaka Y, Kume S, Morita Y, Chin-Kanasaki M, Araki H, Isshiki K, Araki S, Koya D, Haneda M, Kashiwagi A, Maegawa H, Uzu T: Fatty acids are novel nutrient factors to regulate mTORC1 lysosomal localization and apoptosis in podocytes. Biochim Biophys Acta 2014;1842:1097-1108
29. Cohen HY, Miller C, Bitterman KJ, Wall NR, Hekking B, Kessler B, Howitz KT, Gorospe M, de Cabo R, Sinclair DA: Calorie restriction promotes mammalian cell survival by inducing the SIRT1 deacetylase. Science 2004;305:390-392
30. Kume S, Uzu T, Horiike K, Chin-Kanasaki M, Isshiki K, Araki S, Sugimoto T, Haneda M, Kashiwagi A, Koya D: Calorie restriction enhances cell adaptation to hypoxia through Sirt1-dependent mitochondrial autophagy in mouse aged kidney. J Clin Invest 2010;120:1043-1055
31. Mizushima N, Yoshimori T, Levine B: Methods in mammalian autophagy research. Cell 2010;140:313-326
32. Lee GH, Ogawa K, Drinkwater NR: Conditional transformation of mouse liver epithelial cells. An in vitro model for analysis of genetic events in hepatocarcinogenesis. Am J Pathol 1995;147:1811-1822
33. Komatsu M, Waguri S, Ueno T, Iwata J, Murata S, Tanida I, Ezaki J, Mizushima N, Ohsumi Y, Uchiyama Y, Kominami E, Tanaka K, Chiba T: Impairment of starvation-induced and constitutive autophagy in Atg7-deficient mice. J Cell Biol 2005;169:425-434
34. Oliva Trejo JA, Asanuma K, Kim EH, Takagi-Akiba M, Nonaka K, Hidaka T, Komatsu M, Tada N, Ueno T, Tomino Y: Transient increase in proteinuria, poly-ubiquitylated proteins and ER stress markers in podocyte-specific autophagy-deficient mice following unilateral nephrectomy. Biochem Biophys Res Commun 2014;446:1190-1196
35. Takemoto M, Asker N, Gerhardt H, Lundkvist A, Johansson BR, Saito Y, Betsholtz C: A new method for large scale isolation of kidney glomeruli from mice. Am J Pathol 2002;161:799-805
36. Morita S, Kojima T, Kitamura T: Plat-E: an efficient and stable system for transient packaging of retroviruses. Gene Ther 2000;7:1063-1066
37. Pankiv S, Clausen TH, Lamark T, Brech A, Bruun JA, Outzen H, Overvatn A, Bjorkoy G, Johansen T: p62/SQSTM1 binds directly to Atg8/LC3 to facilitate degradation of ubiquitinated protein aggregates by autophagy. J Biol Chem

2007;282:24131-24145
38. Kume S, Uzu T, Araki S, Sugimoto T, Isshiki K, Chin-Kanasaki M, Sakaguchi M, Kubota N, Terauchi Y, Kadowaki T, Haneda M, Kashiwagi A, Koya D: Role of altered renal lipid metabolism in the development of renal injury induced by a high-fat diet. J Am Soc Nephrol 2007;18:2715-2723
39. Kawano K, Hirashima T, Mori S, Saitoh Y, Kurosumi M, Natori T: Spontaneous long-term hyperglycemic rat with diabetic complications. Otsuka Long-Evans Tokushima Fatty (OLETF) strain. Diabetes 1992;41:1422-1428
40. Fukuda H, Hidaka T, Takagi-Akiba M, Ichimura K, Trejo JA, Sasaki Y, Wang J, Sakai T, Asanuma K, Tomino Y: Podocin is translocated to cytoplasm in puromycin aminonucleoside nephrosis rats and in poor-prognosis patients with IgA nephropathy. Cell Tissue Res 2015;
41. Yu L, McPhee CK, Zheng L, Mardones GA, Rong Y, Peng J, Mi N, Zhao Y, Liu Z, Wan F, Hailey DW, Oorschot V, Klumperman J, Baehrecke EH, Lenardo MJ: Termination of autophagy and reformation of lysosomes regulated by mTOR. Nature 2010;465:942-946
42. Tanaka Y, Guhde G, Suter A, Eskelinen EL, Hartmann D, Lullmann-Rauch R, Janssen PM, Blanz J, von Figura K, Saftig P: Accumulation of autophagic vacuoles and cardiomyopathy in LAMP-2-deficient mice. Nature 2000;406:902-906
43. Huber TB, Edelstein CL, Hartleben B, Inoki K, Jiang M, Koya D, Kume S, Lieberthal W, Pallet N, Quiroga A, Ravichandran K, Susztak K, Yoshida S, Dong Z: Emerging role of autophagy in kidney function, diseases and aging. Autophagy 2012;8:1009-1031
44. Hartleben B, Godel M, Meyer-Schwesinger C, Liu S, Ulrich T, Kobler S, Wiech T, Grahammer F, Arnold SJ, Lindenmeyer MT, Cohen CD, Pavenstadt H, Kerjaschki D, Mizushima N, Shaw AS, Walz G, Huber TB: Autophagy influences glomerular disease susceptibility and maintains podocyte homeostasis in aging mice. J Clin Invest 2010;120:1084-1096
45. Kimura T, Takabatake Y, Takahashi A, Kaimori JY, Matsui I, Namba T, Kitamura H, Niimura F, Matsusaka T, Soga T, Rakugi H, Isaka Y: Autophagy protects the proximal tubule from degeneration and acute ischemic injury. J Am Soc Nephrol 2011;22:902-913
46. Liu S, Hartleben B, Kretz O, Wiech T, Igarashi P, Mizushima N, Walz G, Huber TB: Autophagy plays a critical role in kidney tubule maintenance, aging and ischemia-reperfusion injury. Autophagy 2012;8:826-837
47. Takahashi A, Kimura T, Takabatake Y, Namba T, Kaimori J, Kitamura H, Matsui I,

Niimura F, Matsusaka T, Fujita N, Yoshimori T, Isaka Y, Rakugi H: Autophagy guards against cisplatin-induced acute kidney injury. Am J Pathol 2012;180:517-525

48. Kume S, Thomas MC, Koya D: Nutrient sensing, autophagy, and diabetic nephropathy. Diabetes 2012;61:23-29

49. Kim J, Kundu M, Viollet B, Guan KL: AMPK and mTOR regulate autophagy through direct phosphorylation of Ulk1. Nat Cell Biol 2011;13:132-141

50. Godel M, Hartleben B, Herbach N, Liu S, Zschiedrich S, Lu S, Debreczeni-Mor A, Lindenmeyer MT, Rastaldi MP, Hartleben G, Wiech T, Fornoni A, Nelson RG, Kretzler M, Wanke R, Pavenstadt H, Kerjaschki D, Cohen CD, Hall MN, Ruegg MA, Inoki K, Walz G, Huber TB: Role of mTOR in podocyte function and diabetic nephropathy in humans and mice. J Clin Invest 2011;121:2197-2209

51. Inoki K, Mori H, Wang J, Suzuki T, Hong S, Yoshida S, Blattner SM, Ikenoue T, Ruegg MA, Hall MN, Kwiatkowski DJ, Rastaldi MP, Huber TB, Kretzler M, Holzman LB, Wiggins RC, Guan KL: mTORC1 activation in podocytes is a critical step in the development of diabetic nephropathy in mice. J Clin Invest 2011;121:2181-2196

52. Yamahara K, Kume S, Koya D, Tanaka Y, Morita Y, Chin-Kanasaki M, Araki H, Isshiki K, Araki S, Haneda M, Matsusaka T, Kashiwagi A, Maegawa H, Uzu T: Obesity-mediated autophagy insufficiency exacerbates proteinuria-induced tubulointerstitial lesions. J Am Soc Nephrol 2013;24:1769-1781

Figure legends

Figure 1. Autophagy insufficiency in podocytes of diabetic patients with massive proteinuria. (A–C) Representative pictures of periodic acid-Schiff (PAS) staining, immunofluorescent (IF) assays of podocin protein and immunohistochemistry (IHC) for p62, a marker of autophagy insufficiency, in kidney biopsy specimens from patients with diabetic nephropathy (DM) and massive proteinuria (Patients 1–7) or minimal proteinuria (Patients 17–20), membranous nephropathy (MN) with reversible massive proteinuria (Patients 8–13), minimal change nephrotic syndrome (MCNS) (Patients 14–16) and IgA nephropathy (IgA-N) with minimal proteinuria (Patients 21–25). Massive proteinuria was defined as > 3.5 g/day and minimal proteinuria as < 0.5 g/day. Magnification: ×400 for PAS stain and IHC of p62, and ×600 for IF of podocin. (D) Semi-quantitative measurement of p62 intensity in the glomeruli in each group. All results are presented as mean ± SEM, and compared by ANOVA and a subsequent Tukey's test, with $P < 0.05$ considered statistically significant.

Figure 2. Autophagy insufficiency in podocytes of rodent diabetic models with massive proteinuria. (A, B) Western blot analysis of urinary albumin in C57BL/6 mice fed a standard (STD) or a high-fat (HFD) diet (A), and non-diabetic control Long-Evans Tokushima Otsuka (LETO) and diabetic Otsuka Long-Evans Tokushima Fatty (OLETF) rats at the indicated ages (weeks) (B). (C) Representative pictures of periodic acid-Schiff staining (PAS), immunofluorescent (IF) assays of podocin, scanning electron microscopy (EM) and immunohistochemistry (IHC) for p62 in kidneys from C57BL/6 mice fed a STD or a HFD, and LETO and OLETF rats at the indicated ages. Magnifications; × 400 for PAS and IHC of p62, × 1,000 (mouse study) and × 600 (rat study) for IF of podocin, and × 8,000 for scanning EM. (D, E) Semi-quantitative measurement of p62 intensity in glomeruli in each rodent model. All results are presented as mean ± SEM, and compared by ANOVA and a subsequent Tukey's test, with $P < 0.05$ considered statistically significant. NS indicates no significance.

Figure 3. Exacerbation of HFD-induced proteinuria in podocyte-specific autophagy-deficient mice. (A) GFP-LC3-positive dot analysis in podocytes of GFP-LC3 transgenic mice crossbred with either $Atg5^{f/f}$ or podocyte-specific Atg5 knockout (podo-$Atg5^{-/-}$) mice fed ad libitum. Nidogen staining for visualization of basement membrane. White arrow heads indicate GFP-positive autophagosome dots. Magnification; × 1,000. (B, C) Sequential changes in body weight and fasting blood glucose concentrations in the four groups of mice over the 32-week feeding period. (D)

Fasting insulin concentrations in the four groups of mice at the end of the experimental period. (E, F) Glucose change and AUC of glucose concentrations during intraperitoneal glucose tolerance tests (IPGTT). (G, H) Glucose change and AUC of glucose concentrations during intraperitoneal insulin tolerance tests (IPITT). (I) Western blot analysis of albumin in urine samples from the four groups of mice at the end of the experimental period. (J) Urinary albumin excretion levels by ELISA at 0 and 32 weeks. All values are shown as mean ± SEM, with levels of significance determined by ANOVA and a subsequent Tukey's test. *$P < 0.05$ vs. $Atg5^{f/f}$ mice fed STD. †$P < 0.01$ vs. $Atg5^{-/-}$ mice fed STD. **$P < 0.01$ and ***$P < 0.05$ vs. the indicated groups. NS indicates no significance. STD: standard diet, HFD: high fat diet, AUC: area under the curve, ELISA: Enzyme-linked immunosorbent assay.

Figure 4. Exacerbation of proteinuria-related tubulointerstitial lesions in HFD-fed podocyte-specific autophagy-deficient mice. (A) Representative pictures of periodic acid-Schiff (PAS) staining and immunohistochemical expression of fibronectin in glomeruli of four groups of mice. Magnification; × 400. (B) Quantitative analysis of glomerular size and fibronectin positive areas in glomeruli. (C) Quantitative evaluation of tubulointerstitial lesions by H&E staining and immunohistochemical analysis of F4/80. Magnification; × 200. (D) Tubular damage scores by H&E staining and F4/80-positive scores. (E) Representative pictures of immunohistochemical assays for p62. Magnification; × 400. (F) Quantitation of the numbers of p62-positive cells in the glomeruli of the four groups of mice. (G, H) GFP-LC3 dot analysis of GFP-LC3 transgenic mice fed a STD or a HFD for 32 weeks. Representative pictures of the glomeruli from GFP-LC3 transgenic mice fed the indicated diet (G) and quantitation of numbers of GFP-dots in the glomeruli (H) (n = 4). Magnification; × 1,000. All values are presented as mean ± SEM, with statistical significance determined by ANOVA and subsequent Tukey's tests for multiple comparisons and by Student's t tests for pairwise comparisons. *$P < 0.05$. **$P < 0.01$ vs. the indicated groups. NS indicates no significance.

Figure 5. Podocyte dysfunction and loss in HFD-fed podocyte-specific autophagy deficient mice. Representative transmission (A) and scanning (B) electron microscopy of glomeruli from $Atg5^{f/f}$ and $Atg5^{-/-}$ mice fed a standard (STD) or a high-fat diet (HFD) for 32 weeks. The asterisk indicates thickening of the glomerular basement membrane. Magnification; × 10,000 for transmission electron microscopy and × 8,000 for scanning electron microscopy. (C) Immunofluorescent determination of podocin

expression in glomeruli from the four groups of mice. Magnification; × 1,000. (D) Double immunofluorescent determination of podocin and synaptopodin in glomeruli from the four groups of mice. Magnification; × 1,000. The red- and green-colored lines represent podocin and synaptopodin, respectively. Under normal conditions, both proteins are visible as capillary pattern. Once podocyte damage occurs, podocin is internalized, making yellow lines and red-colored dots in cytosol. (E) Representative pictures of WT1 stain in glomeruli of the four groups of mice. Magnification; × 400. (F) Quantitation of WT1-positive podocytes in glomeruli. All values are presented as mean ± SEM. Differences were determined by ANOVA and a subsequent Tukey's test. *P < 0.05 vs. the indicated groups.

Figure 6. Autophagy insufficiency and apoptosis in cultured podocytes stimulated with serum from diabetic rodent models. (A) Representative western blots for p62, β actin and LC3 in cultured normal podocytes incubated with high glucose (500 mg/dl), fatty acids (palmitate and oleate, 150 μM each), TNFα or all three reagents (triple). (B, C) Quantitative ratios of p62 to β actin (B) and of LC3II to LC3I (C) (n = 3). (D) Study protocols 1–4 for cell culture with sera from the indicated non-diabetic and diabetic rodents. (E) Representative pictures of LC3 immunofluorescence in cultured normal podocytes incubated with 10% serum from the rodents indicated in protocol 1. (F) Representative western blots for p62, cleaved caspase 3, β actin and LC3 in cultured normal podocytes incubated with 10% serum of the rats indicated in protocol 2. (G) Quantitative ratios of p62, cleaved caspase 3 to β actin and ratio of LC3II to LC3I (n = 3). (H) Representative western blots for p62 and cleaved caspase 3 in cultured normal podocytes incubated with 10% serum of $Atg5^{f/f}$ mice fed a STD or Atg5-deficient mice fed a HFD indicated in protocol 3. (I) Representative western blots of Atg7, p62, cleaved caspase 3, β actin and LC3 in cultured $Atg7^{f/f}$ and Atg7-deficient podocytes incubated with 10% sera from the mice indicated in protocol 4. (J) Quantitative ratios of p62 and cleaved caspase 3 to β actin (n = 3). All values are presented as mean ± SEM. ANOVA and a subsequent Tukey's test were used to determine significance in multiple comparisons, whereas Student's t test was used for pairwise comparisons. $P < 0.05$ was considered statistically significant. STD: standard diet, HFD: high fat diet. TNFα: tomor necrotic factor α.

Figure 7. Damaged lysosomes in podocytes of diabetic rodent models with massive proteinuria. (A) Representative transmission electron microscopy pictures of podocytes from $Atg5^{f/f}$ and $Atg5^{-/-}$ mice fed a standard (STD) or a high-fat diet (HFD)

for 32 weeks. Magnification; × 20,000. (B) Hypothetic schema showing that some diabetes conditions increase metabolic loads to lysosomes, requiring damaged lysosome to be removed by autophagy (lysophagy) and eventually degraded in residual normal lysosomes. (C) Immunofluorescent expression of lamp2, a lysosome membrane marker, and ubiquitinated proteins in the glomeruli of the four groups of mice. Magnification; × 1,000. Yellow arrow heads; ubiquitin-positive cells. (D) Representative transmission electron microscopy pictures of podocytes and immunofluorescent expression of lamp2 in 50-week-old Long-Evans Tokushima (LETO) and Otsuka Long-Evans Tokushima Fatty (OLETF) rats. Magnification; × 15,000 for electron microscopy and × 600 for lamp2. (E) Western blot analysis of ubiquitinated proteins in cultured $Atg7^{f/f}$ and $Atg7^{-/-}$ podocytes incubated with 10% serum from C57BL/6 mice fed a STD or a HFD, and from 50-week-old LETO and OLETF rats. (F, G) Double immunofluorescent assay for LC3 and lamp2 in the indicated cells. Magnification; × 1,000.

Figure 8. Autophagy-lysosome dysfunction and apoptosis in cultured podocytes stimulated with sera from diabetic patients with massive proteinuria. (A) Representative western blot analyses of p62, ubiquitinated proteins and β actin in cultured podocytes incubated with sera from type 2 diabetic patients with normo (n = 3), micro (n = 3), macro (n = 2) and massive albuminuria (n = 3). (B) Protocol of the cell culture experiment. Cultured normal podocytes were incubated with the sera from non-diabetic subjects (n = 10), and diabetic patients with normo (n = 10), micro (n = 11), macro (n = 10) and massive albuminuria (n = 9). The collected cell lysates were analyzed by ELISA for expression of p62 protein. (C) Result of p62 ELISA. All results are presented as mean ± SEM, and compared by ANOVA and a subsequent Tukey's test, with $P < 0.05$ considered statistically significant. (D) Hypothetic schema of the present study. Diabetic conditions alone result in mild glomerular lesions with minimal proteinuria. During disease development, however, the combination of insufficient podocyte autophagy and diabetes results in podocyte loss and foot process alteration with lysosome dysfunction, which is associated with the pathogenesis of massive proteinuria.

Figure 1

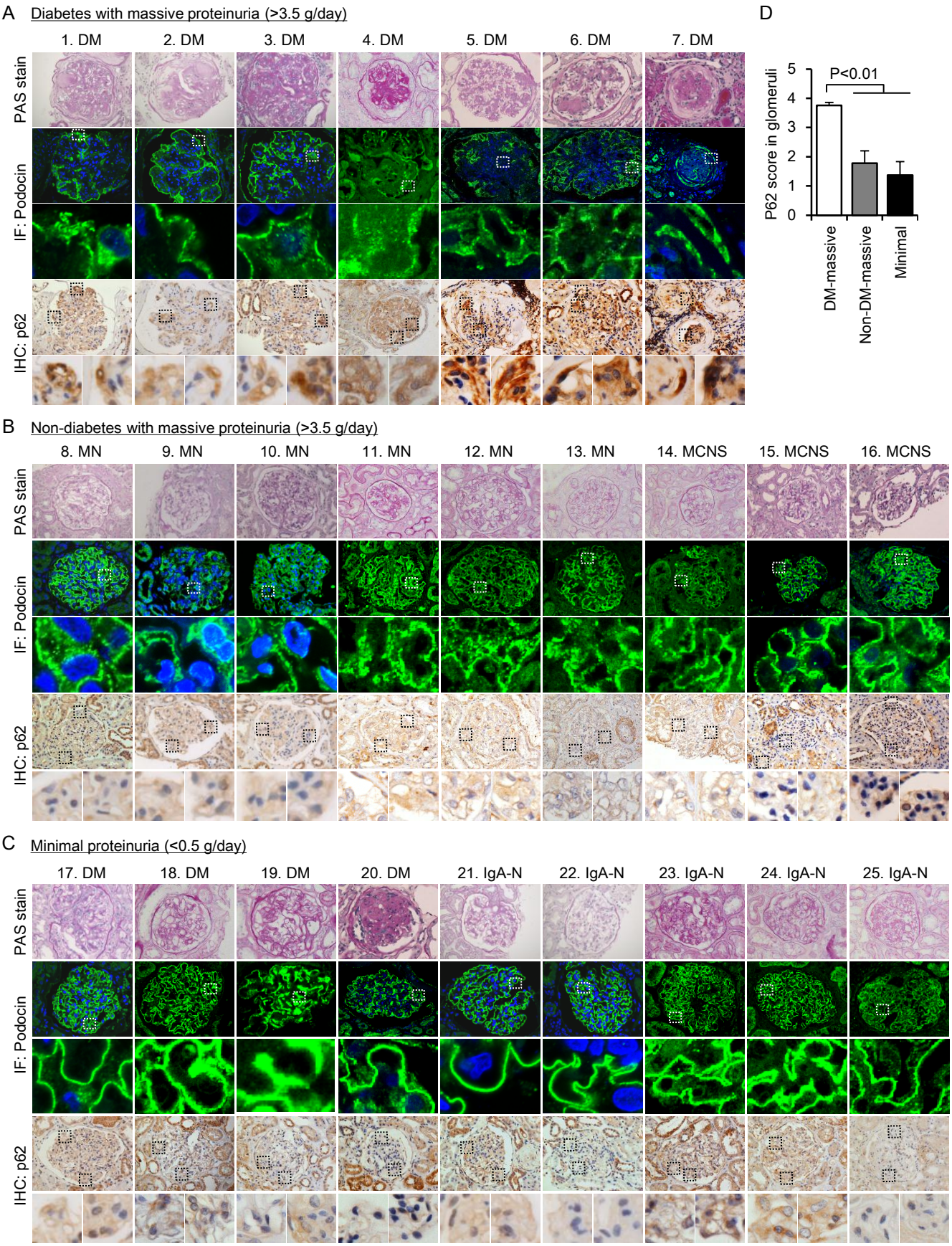
A
Diabetes with massive proteinuria (>3.5 g/day)
1. DM
2. DM
3. DM
4. DM
5. DM
6. DM
7. DM
PAS stain
IF: Podocin
IHC: p62
B
Non-diabetes with massive proteinuria (>3.5 g/day)
8. MN
9. MN
10. MN
11. MN
12. MN
13. MN
14. MCNS
15. MCNS
16. MCNS
C
Minimal proteinuria (<0.5 g/day)
17. DM
18. DM
19. DM
20. DM
21. IgA-N
22. IgA-N
23. IgA-N
24. IgA-N
25. IgA-N
D
P62 score in glomeruli
P<0.01
DM-massive
Non-DM-massive
Minimal

Figure 2

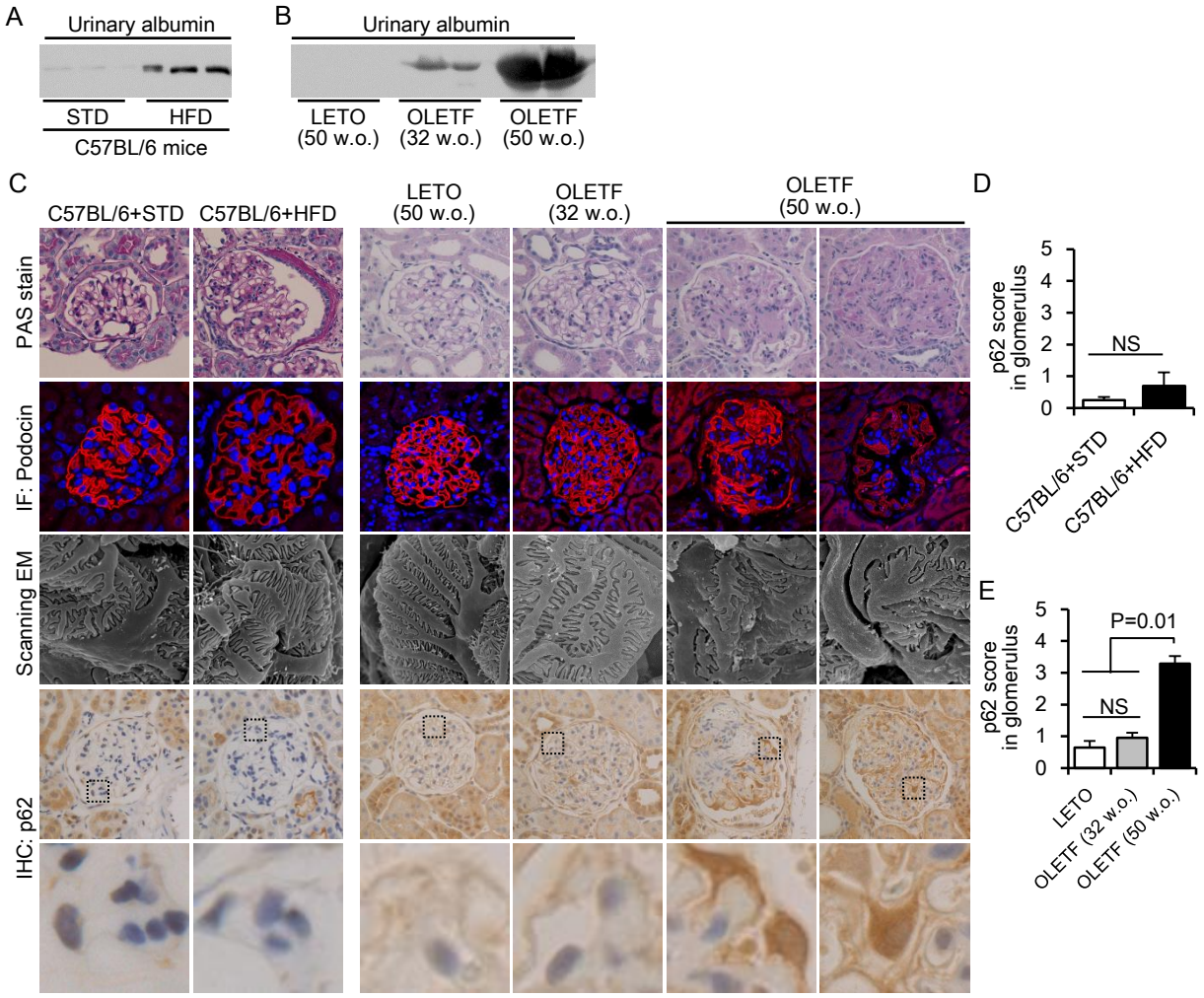
A
Urinary albumin
STD
HFD
C57BL/6 mice
B
Urinary albumin
LETO (50 w.o.)
OLETF (32 w.o.)
OLETF (50 w.o.)
C
C57BL/6+STD
C57BL/6+HFD
LETO (50 w.o.)
OLETF (32 w.o.)
OLETF (50 w.o.)
PAS stain
IF: Podocin
Scanning EM
IHC: p62
D
p62 score in glomerulus
NS
C57BL/6+STD
C57BL/6+HFD
E
p62 score in glomerulus
P=0.01
NS
LETO
OLETF (32 w.o.)
OLETF (50 w.o.)

Figure 3

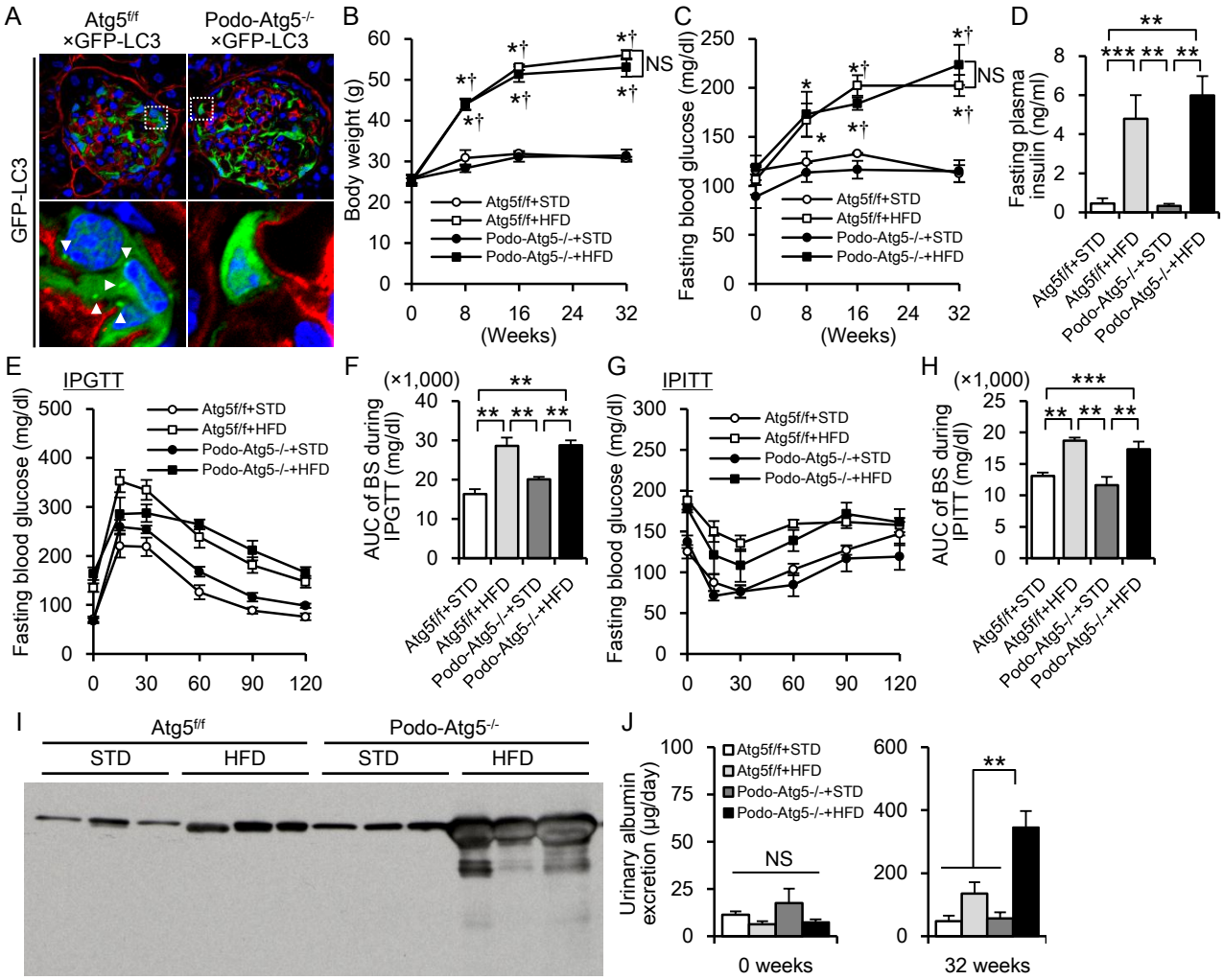
A
Atg5f/f ×GFP-LC3
Podo-Atg5-/- ×GFP-LC3
GFP-LC3
B
Body weight (g)
(Weeks)
NS
Atg5f/f+STD
Atg5f/f+HFD
Podo-Atg5-/-+STD
Podo-Atg5-/-+HFD
C
Fasting blood glucose (mg/dl)
(Weeks)
NS
D
Fasting plasma insulin (ng/ml)
E
IPGTT
Fasting blood glucose (mg/dl)
F
(×1,000)
AUC of BS during IPGTT (mg/dl)
G
IPITT
Fasting blood glucose (mg/dl)
H
(×1,000)
AUC of BS during IPITT (mg/dl)
I
Atg5f/f
Podo-Atg5-/-
STD
HFD
STD
HFD
J
Urinary albumin excretion (μg/day)
NS
0 weeks
32 weeks

Figure 4

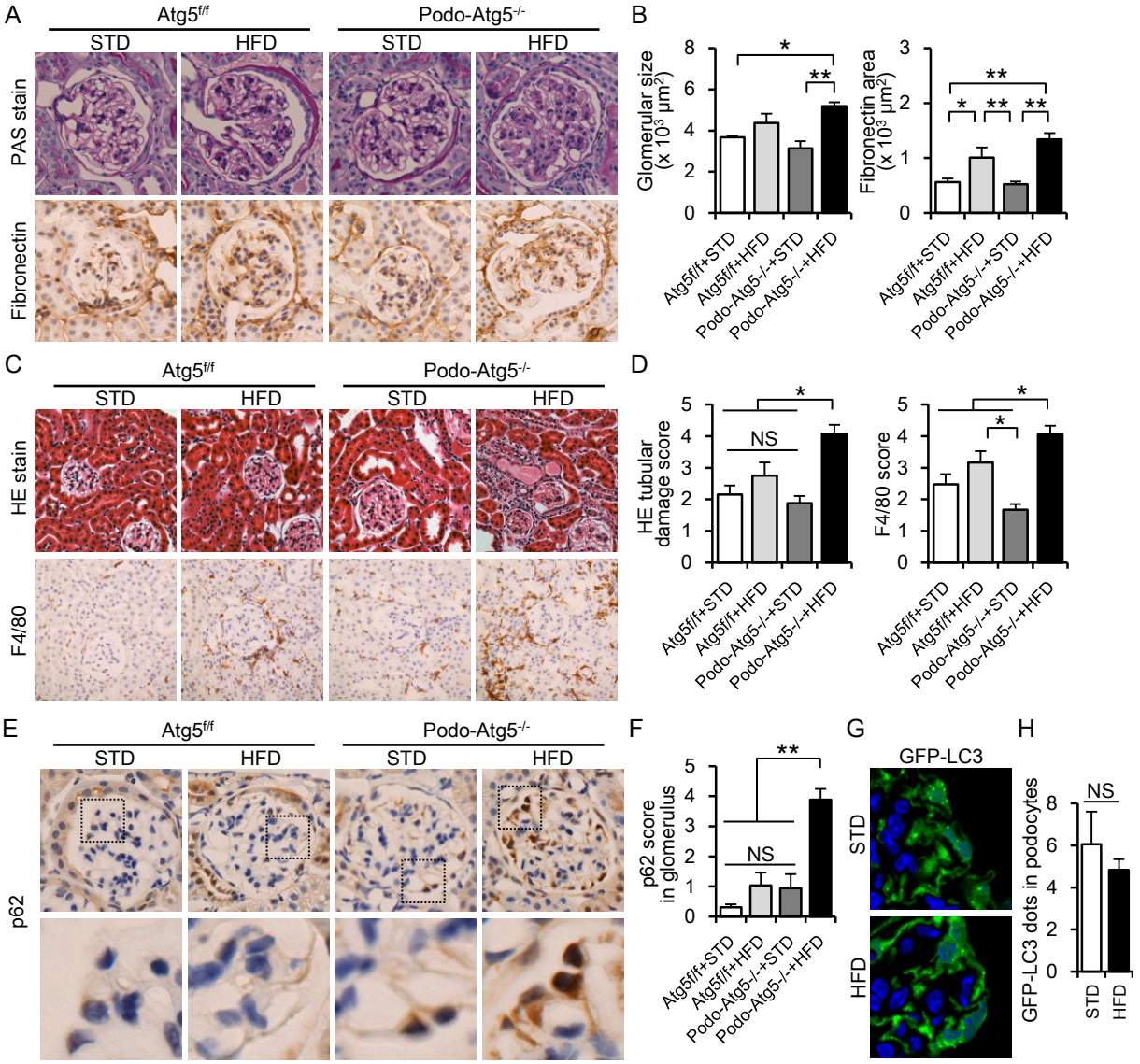
A
Atg5f/f
Podo-Atg5-/-
STD
HFD
STD
HFD
PAS stain
Fibronectin
B
Glomerular size (x 10³ μm²)
Fibronectin area (x 10³ μm²)
Atg5f/f+STD
Atg5f/f+HFD
Podo-Atg5-/-+STD
Podo-Atg5-/-+HFD
C
HE stain
F4/80
D
HE tubular damage score
F4/80 score
NS
E
p62
F
p62 score in glomerulus
G
GFP-LC3
STD
HFD
H
GFP-LC3 dots in podocytes

Figure 5

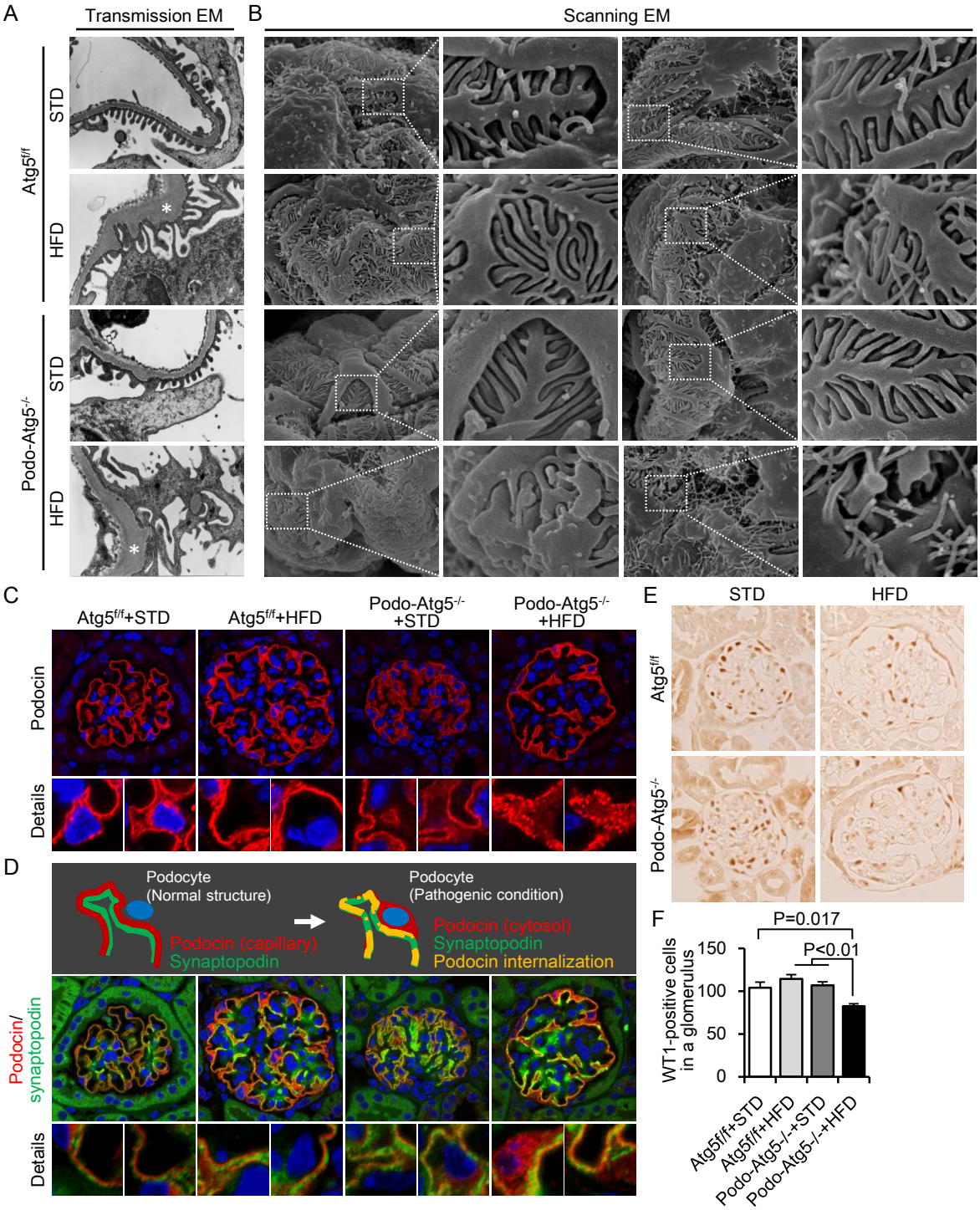
A
Transmission EM
B
Scanning EM
Atg5f/f
STD
HFD
Podo-Atg5-/-
STD
HFD
C
Atg5f/f+STD
Atg5f/f+HFD
Podo-Atg5-/- +STD
Podo-Atg5-/- +HFD
Podocin
Details
D
Podocyte (Normal structure)
Podocin (capillary)
Synaptopodin
Podocyte (Pathogenic condition)
Podocin (cytosol)
Synaptopodin
Podocin internalization
Podocin/ synaptopodin
Details
E
STD
HFD
Atg5f/f
Podo-Atg5-/-
F
P=0.017
P<0.01
WT1-positive cells in a glomerulus
150
100
50
0
Atg5f/f+STD
Atg5f/f+HFD
Podo-Atg5-/-+STD
Podo-Atg5-/-+HFD

Figure 6

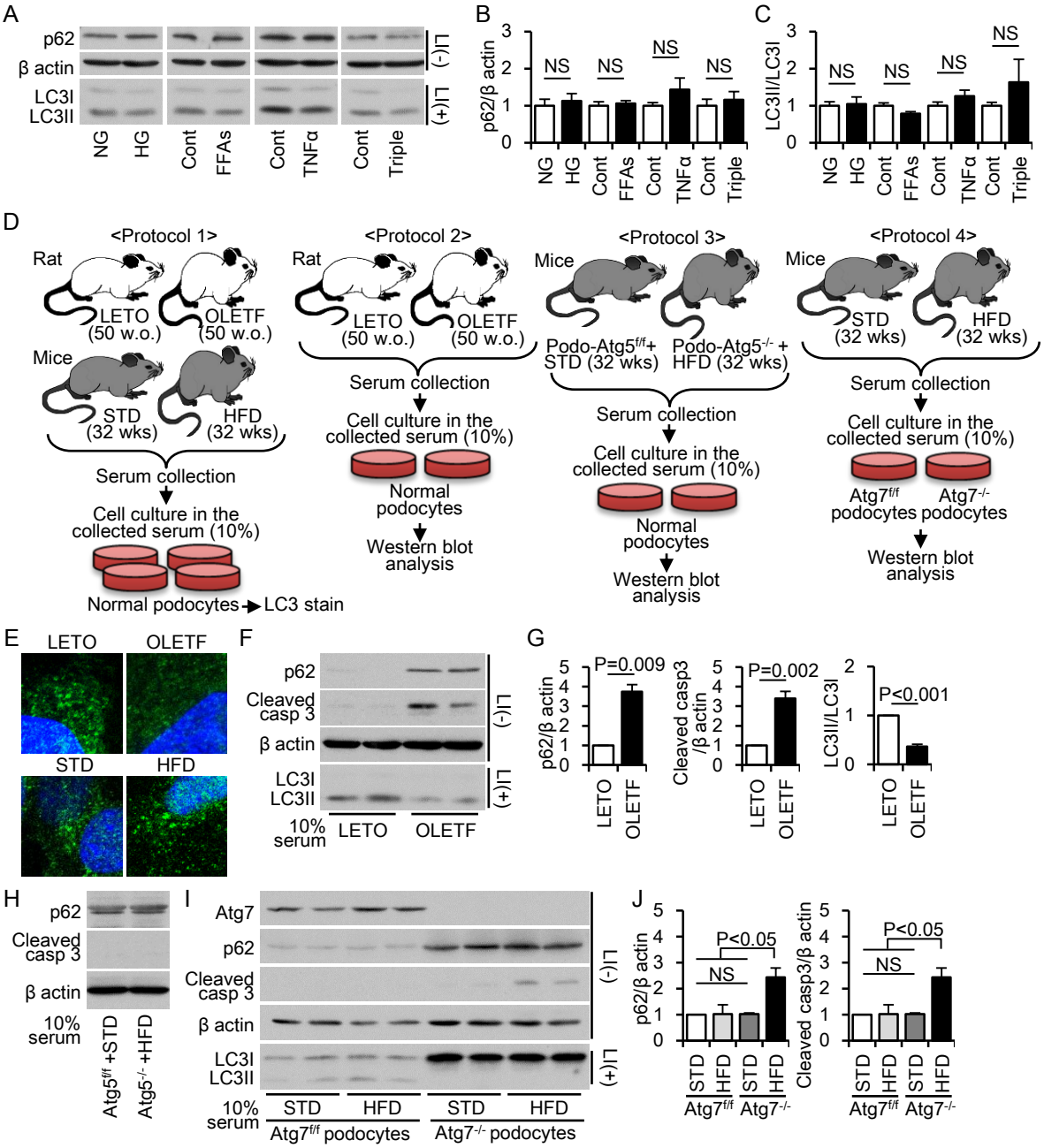
A
p62
β actin
LC3I
LC3II
LI(-)
LI(+)
NG
HG
Cont
FFAs
Cont
TNFα
Cont
Triple
B
p62/β actin
NS
C
LC3II/LC3I
NS
D
<Protocol 1>
Rat
LETO (50 w.o.)
OLETF (50 w.o.)
Mice
STD (32 wks)
HFD (32 wks)
Serum collection
Cell culture in the collected serum (10%)
Normal podocytes
LC3 stain
<Protocol 2>
Western blot analysis
<Protocol 3>
Podo-Atg5f/f+ STD (32 wks)
Podo-Atg5-/- + HFD (32 wks)
<Protocol 4>
Atg7f/f podocytes
Atg7-/- podocytes
E
LETO
OLETF
STD
HFD
F
p62
Cleaved casp 3
β actin
LC3I
LC3II
10% serum
G
P=0.009
Cleaved casp3 /β actin
P=0.002
P≤0.001
H
I
Atg7
Atg5f/f +STD
Atg5-/- +HFD
Atg7f/f podocytes
Atg7-/- podocytes
J
P<0.05

Figure 7

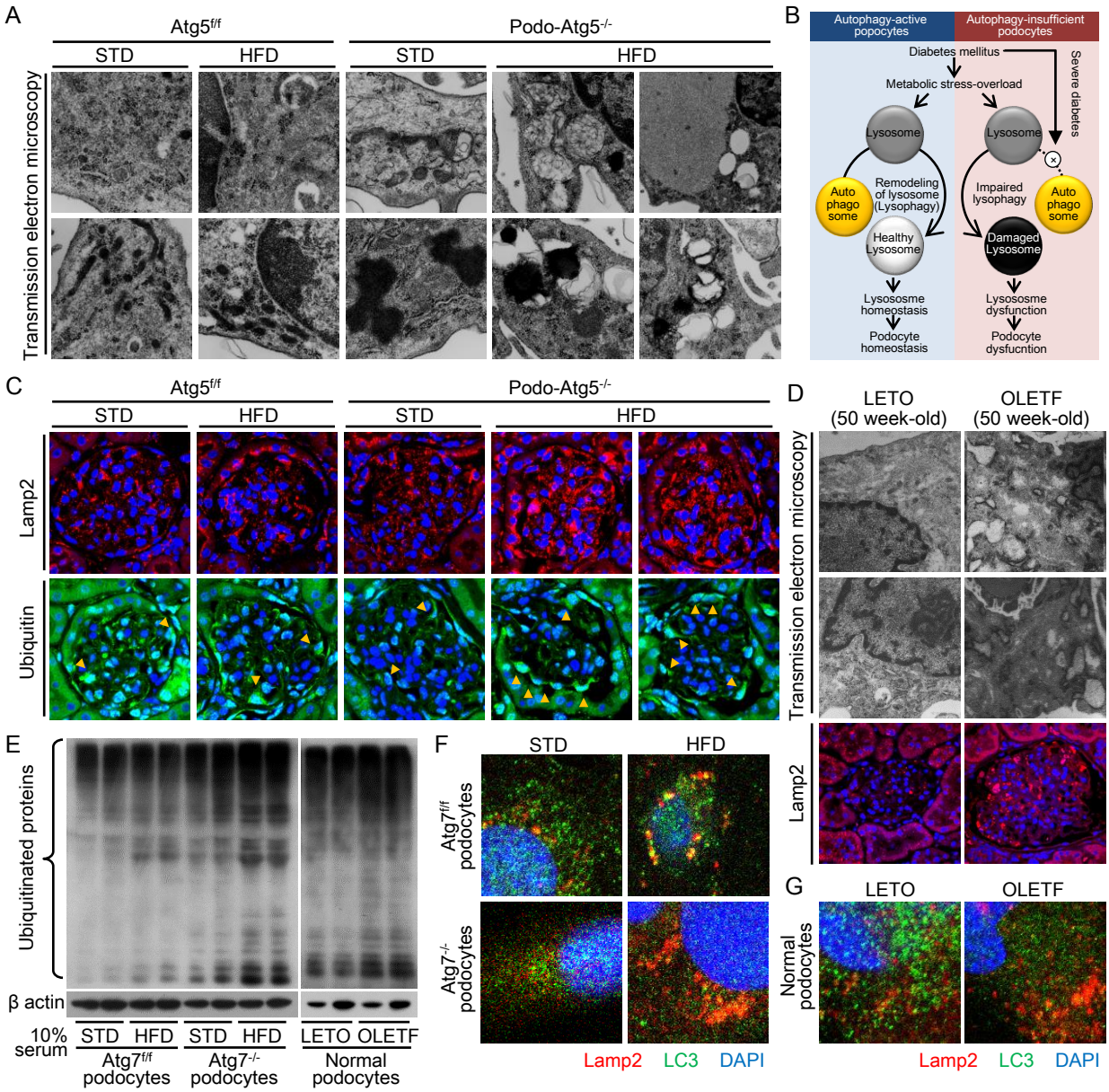
A
Atg5f/f
Podo-Atg5-/-
STD
HFD
STD
HFD
Transmission electron microscopy
B
Autophagy-active popocytes
Autophagy-insufficient podocytes
Diabetes mellitus
Metabolic stress-overload
Severe diabetes
Lysosome
Lysosome
Auto phago some
Remodeling of lysosome (Lysophagy)
Impaired lysophagy
Auto phago some
Healthy Lysosome
Damaged Lysosome
Lysososme homeostasis
Lysososme dysfunction
Podocyte homeostasis
Podocyte dysfucntion
C
Atg5f/f
Podo-Atg5-/-
STD
HFD
STD
HFD
Lamp2
Ubiquitin
D
LETO (50 week-old)
OLETF (50 week-old)
Transmission electron microscopy
Lamp2
E
Ubiquitinated proteins
β actin
10% serum
STD
HFD
STD
HFD
LETO
OLETF
Atg7f/f podocytes
Atg7-/- podocytes
Normal podocytes
F
STD
HFD
Atg7f/f podocytes
Atg7-/- podocytes
Lamp2
LC3
DAPI
G
LETO
OLETF
Normal podocytes
Lamp2
LC3
DAPI

Figure 8

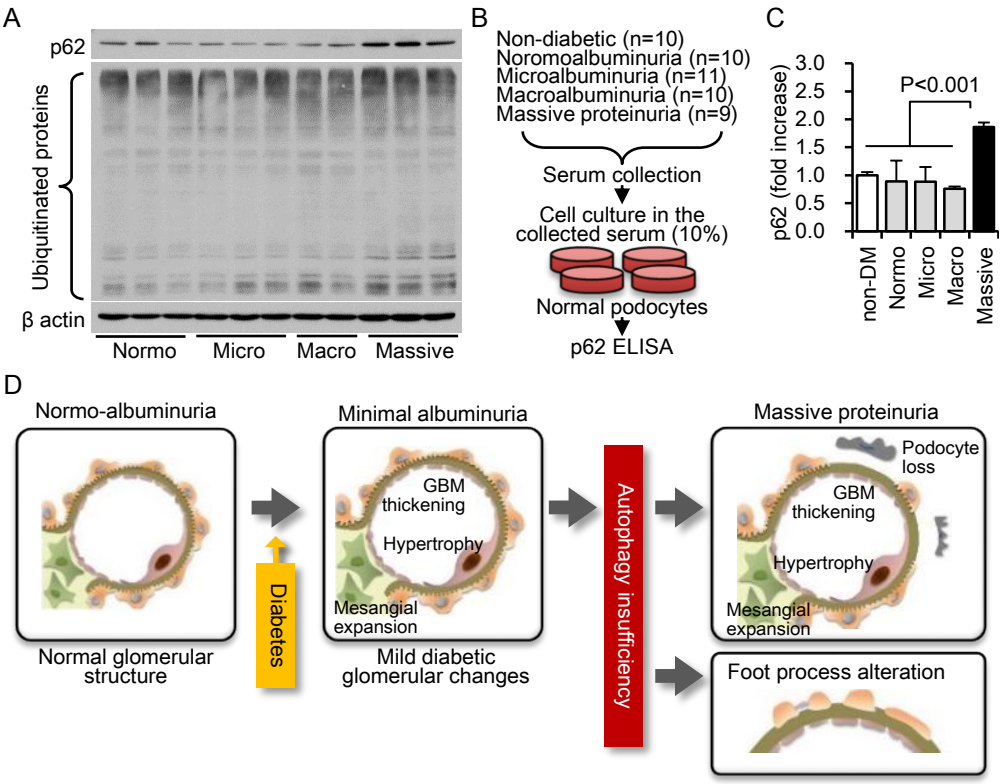
A
p62
Ubiquitinated proteins
β actin
Normo
Micro
Macro
Massive
B
Non-diabetic (n=10)
Noromoalbuminuria (n=10)
Microalbuminuria (n=11)
Macroalbuminuria (n=10)
Massive proteinuria (n=9)
Serum collection
Cell culture in the collected serum (10%)
Normal podocytes
p62 ELISA
C
p62 (fold increase)
3.0
2.5
2.0
1.5
1.0
0.5
0.0
P<0.001
non-DM
Normo
Micro
Macro
Massive
D
Normo-albuminuria
Normal glomerular structure
Diabetes
Minimal albuminuria
GBM thickening
Hypertrophy
Mesangial expansion
Mild diabetic glomerular changes
Autophagy insufficiency
Massive proteinuria
Podocyte loss
GBM thickening
Hypertrophy
Mesangial expansion
Foot process alteration

Supplemental Table 1

	Mice fed with ND	Mice fed with HFD	P value	50 week-old LETO rats	50 week-old OLETF rats	P value
Body weight (g)	32.2 ± 0.73	50.6 ± 1.35	< 0.01	553.3 ± 3.33	720.0 ± 23.1	< 0.01
Glucose (mg/dl)	161.0 ± 13.1	288.5 ± 22.9	< 0.01	141.0 ± 1.00	321.3 ± 2.67	< 0.01
Triglyceride (mg/dl)	80.0 ± 6.03	104.5 ± 7.00	< 0.05	212.7 ± 66.0	513.2 ± 6.28	< 0.01

Supplemental Table 1. Characteristics of animal and sera used in cell culture. Student's t-tests were used for statistical analyses, with $P < 0.05$ considered statistically significant. STD, standard diet; HFD, high-fat diet; LETO, Long-Evans Tokushima Otsuka; OLETF, Otsuka Long-Evans Tokushima Fatty

Supplemental Table 2

Stage	No.	Age (Years old)	Duration (Years)	HbA1c (NGSP; %)	UALB /UCRE (mg/gCre)	UTP /UCRE (g/gCre)	Glu (mg/dl)	LDL (mg/dl)	HDL (mg/dl)	SBP (mmHg)	RAS blocker use
Non-diabetic (n=10)	1	31	0	5.1	ND	ND	89	ND	ND	118	-
	2	35	0	5.1	ND	ND	78	ND	ND	124	-
	3	23	0	4.7	ND	ND	98	ND	ND	107	-
	4	39	0	5.0	ND	ND	99	ND	ND	112	-
	5	55	0	5.8	ND	ND	110	ND	ND	121	-
	6	24	0	5.6	ND	ND	88	ND	ND	107	-
	7	50	0	5.3	ND	ND	98	ND	ND	130	-
	8	35	0	5.6	ND	ND	87	ND	ND	101	-
	9	46	0	5.1	ND	ND	87	ND	ND	133	-
	10	51	0	4.7	ND	ND	97	ND	ND	112	-
Normo (n=10)	11	67	31	6.8	2.3	0.04	168	144	63	121	-
	12	63	28	7.9	5.1	0.05	163	118	44	140	+
	13	68	25	7.8	5.4	0.04	161	152	42	151	+
	14	62	32	7.2	6.7	0.04	174	132	46	110	-
	15	56	26	7.9	19.1	0.04	204	66	79	151	+
	16	58	23	8.5	1.0	0.01	202	84	42	133	+
	17	73	20	7.3	2.7	0.04	92	85	49	137	+
	18	78	24	7.4	4.2	0.03	119	152	42	151	+
	19	62	26	7.9	5.7	0.02	132	124	55	121	+
	20	65	31	8.6	6.4	0.03	151	102	48	121	+
Micro (n=11)	21	76	36	7.2	57.7	0.12	152	108	29	143	+
	22	75	30	7.7	63.4	0.16	125	128	32	128	+
	23	62	22	7.7	87.9	0.24	163	140	60	129	+
	24	75	20	8.1	139.6	0.20	116	118	36	138	+
	25	71	21	7.1	192.3	0.25	134	106	39	148	+
	26	69	27	7.3	34.7	0.07	159	119	56	122	-
	27	57	27	8.2	36.7	0.07	169	84	77	151	+
	28	72	32	7.6	44.8	0.09	189	152	49	137	-
	29	72	32	7.6	49.3	0.13	201	95	92	157	+
	30	62	22	8.1	16.6	0.04	124	142	77	151	-
	31	65	40	8.0	73.8	0.12	187	98	45	112	-
Macro (n=10)	32	59	29	7.2	338.5	0.38	145	108	53	126	+
	33	78	10	8.1	475.3	0.64	82	89	57	157	+
	34	59	42	8.9	585.7	0.72	170	106	33	117	+
	35	71	28	6.7	789.8	0.90	144	80	58	132	+
	36	57	18	8.2	985.7	1.52	118	99	36	158	+
	37	79	24	7.2	467.0	0.57	131	107	58	158	-
	38	54	12	6.9	810.6	1.31	90	43	27	138	+
	39	68	23	6.4	819.0	0.96	97	147	58	169	+
	40	56	16	9.0	1284.0	1.75	200	55	29	129	+
	41	70	19	7.0	2034.2	2.65	181	175	45	143	-

Massive (n=9)	42	80	25	7.1	2937.2	4.56	109	96	77	148	+
	43	67	25	6.7	3702.8	5.00	117	145	80	172	-
	44	62	24	7.0	4207.0	5.48	148	127	63	148	+
	45	72	37	5.4	4505.3	5.78	117	174	55	155	-
	46	47	20	7.0	9609.4	19.30	171	76	36	134	+
	47	54	27	9.7	2630.0	3.82	347	78	28	162	+
	48	64	14	7.0	3401.3	4.70	123	92	46	161	+
	49	57	23	11.2	3785.2	5.78	107	143	67	171	+
	50	72	22	5.9	4870.3	7.35	146	127	48	184	-

Supplemental Table 2. Clinical characteristics in 10 non-diabetic subjects and 40 diabetic patients with normoalbuminuria (< 30 mg/gCre; n = 10), microalbuminuria (30-300 mg/gCre; n = 11), macroalbuminuria (> 300 mg/gCre; n = 10) and massive proteinuria (> 3.5 g/gCre; n = 9). UALB; urinary albumin concentration, UCRE; urinary creatinine concentration, Glu; glucose, LDL; low-density lipoprotein, HDL; high-density lipoprotein, SBP; systolic blood pressure, RAS; renin angiotensin system, ELISA; enzyme-linked immunosorbent assay. ND indicates not determined.

SUPPLEMENTARY DATA

Supplementary Table 1. Characteristics of animal and sera used in cell culture. Student's t-tests were used for statistical analyses, with $P < 0.05$ considered statistically significant. STD, standard diet; HFD, high-fat diet; LETO, Long-Evans Tokushima Otsuka; OLETF, Otsuka Long-Evans Tokushima Fatty

	Mice fed with ND	Mice fed with HFD	P value	50 week-old LETO rats	50 week-old OLETF rats	P value
Body weight (g)	32.2 ± 0.73	50.6 ± 1.35	< 0.01	553.3 ± 3.33	720.0 ± 23.1	< 0.01
Glucose (mg/dl)	161.0 ± 13.1	288.5 ± 22.9	< 0.01	141.0 ± 1.00	321.3 ± 2.67	< 0.01
Triglyceride (mg/dl)	80.0 ± 6.03	104.5 ± 7.00	< 0.05	212.7 ± 66.0	513.2 ± 6.28	< 0.01

SUPPLEMENTARY DATA

Supplementary Table 2. Clinical characteristics in 10 non-diabetic subjects and 40 diabetic patients with normoalbuminuria (< 30 mg/gCre; n = 10), microalbuminuria (30-300 mg/gCre; n = 11), macroalbuminuria (> 300 mg/gCre; n = 10) and massive proteinuria (> 3.5 g/gCre; n = 9). UALB; urinary albumin concentration, UCRE; urinary creatinine concentration, Glu; glucose, LDL; low-density lipoprotein, HDL; high-density lipoprotein, SBP; systolic blood pressure, RAS; renin angiotensin system, ELISA; enzyme-linked immunosorbent assay. ND indicates not determined.

Stage	No.	Age (Years old)	Duration (Years)	HbA1c (NGSP; %)	UALB /UCRE (mg/gCre)	UTP /UCRE (g/gCre)	Glu (mg/dl)	LDL (mg/dl)	HDL (mg/dl)	SBP (mmHg)	RAS blocker use
Non-diabetic (n=10)	1	31	0	5.1	ND	ND	89	ND	ND	118	-
	2	35	0	5.1	ND	ND	78	ND	ND	124	-
	3	23	0	4.7	ND	ND	98	ND	ND	107	-
	4	39	0	5.0	ND	ND	99	ND	ND	112	-
	5	55	0	5.8	ND	ND	110	ND	ND	121	-
	6	24	0	5.6	ND	ND	88	ND	ND	107	-
	7	50	0	5.3	ND	ND	98	ND	ND	130	-
	8	35	0	5.6	ND	ND	87	ND	ND	101	-
	9	46	0	5.1	ND	ND	87	ND	ND	133	-
	10	51	0	4.7	ND	ND	97	ND	ND	112	-
Normo (n=10)	11	67	31	6.8	2.3	0.04	168	144	63	121	-
	12	63	28	7.9	5.1	0.05	163	118	44	140	+
	13	68	25	7.8	5.4	0.04	161	152	42	151	+
	14	62	32	7.2	6.7	0.04	174	132	46	110	-
	15	56	26	7.9	19.1	0.04	204	66	79	151	+
	16	58	23	8.5	1.0	0.01	202	84	42	133	+
	17	73	20	7.3	2.7	0.04	92	85	49	137	+
	18	78	24	7.4	4.2	0.03	119	152	42	151	+
	19	62	26	7.9	5.7	0.02	132	124	55	121	+
	20	65	31	8.6	6.4	0.03	151	102	48	121	+
Micro (n=11)	21	76	36	7.2	57.7	0.12	152	108	29	143	+
	22	75	30	7.7	63.4	0.16	125	128	32	128	+
	23	62	22	7.7	87.9	0.24	163	140	60	129	+
	24	75	20	8.1	139.6	0.20	116	118	36	138	+
	25	71	21	7.1	192.3	0.25	134	106	39	148	+
	26	69	27	7.3	34.7	0.07	159	119	56	122	-
	27	57	27	8.2	36.7	0.07	169	84	77	151	+
	28	72	32	7.6	44.8	0.09	189	152	49	137	-
	29	72	32	7.6	49.3	0.13	201	95	92	157	+
	30	62	22	8.1	16.6	0.04	124	142	77	151	-
	31	65	40	8.0	73.8	0.12	187	98	45	112	-
Macro (n=10)	32	59	29	7.2	338.5	0.38	145	108	53	126	+
	33	78	10	8.1	475.3	0.64	82	89	57	157	+
	34	59	42	8.9	585.7	0.72	170	106	33	117	+
	35	71	28	6.7	789.8	0.90	144	80	58	132	+

SUPPLEMENTARY DATA

	36	57	18	8.2	985.7	1.52	118	99	36	158	+
	37	79	24	7.2	467.0	0.57	131	107	58	158	-
	38	54	12	6.9	810.6	1.31	90	43	27	138	+
	39	68	23	6.4	819.0	0.96	97	147	58	169	+
	40	56	16	9.0	1284.0	1.75	200	55	29	129	+
	41	70	19	7.0	2034.2	2.65	181	175	45	143	-
Massive (n=9)	42	80	25	7.1	2937.2	4.56	109	96	77	148	+
	43	67	25	6.7	3702.8	5.00	117	145	80	172	-
	44	62	24	7.0	4207.0	5.48	148	127	63	148	+
	45	72	37	5.4	4505.3	5.78	117	174	55	155	-
	46	47	20	7.0	9609.4	19.30	171	76	36	134	+
	47	54	27	9.7	2630.0	3.82	347	78	28	162	+
	48	64	14	7.0	3401.3	4.70	123	92	46	161	+
	49	57	23	11.2	3785.2	5.78	107	143	67	171	+
	50	72	22	5.9	4870.3	7.35	146	127	48	184	-